Monocyclic Human Tachykinin NK-2 Receptor Antagonists as Evolution of a Potent Bicyclic Antagonist: QSAR and Site-Directed Mutagenesis Studies

Alessandro Giolitti,*,[†] Maria Altamura,[‡] Francesca Bellucci,[§] Danilo Giannotti,[‡] Stefania Meini,[§] Riccardo Patacchini,[§] Luigi Rotondaro,[‖] Sabrina Zappitelli,[‖] and Carlo A. Maggi[§]

Departments of Drug Design, Chemistry, Pharmacology, and Biotechnology, Menarini Ricerche S.p.A., Via Sette Santi 3, 50131 Firenze, Italy

A new series of monocyclic pseudopeptidic tachykinin NK-2 receptor antagonists has been derived from nepadutant with the help of site-directed mutagenesis studies and QSAR models. MEN11558 is the lead compound which is evaluated on a series of 13 new human tachykinin NK-2 receptor mutants (Tyr107Ala, Gln109Ala, Asn110Ala, Phe112Ala, Ser164Phe, Cys167Gly, Phe168Ala, Tyr169Ala, Ile202Phe, Trp263Ala, Tyr269Phe, Tyr269Ala, and Phe293Ala) and 8 mutants on which data from nepadutant were already available (Gln166Ala, Ser170Ala, Thr171Ala, His198Ala, Tyr206Phe, Tyr266Phe, Tyr289Phe, and Tyr289Thr). The results show that the two compounds share most of their binding sites, in agreement with their hypothesized binding modes. This allows us to transfer the structural knowledge we already had for nepadutant to the new series of compounds. At the same time, a sound QSAR model is developed to assist the prioritization of new chemical syntheses. The result is the discovery of receptor antagonists with a higher affinity than nepadutant for the hNK-2 receptor.

Introduction

Neurokinin A, a member of the tachykinin peptide family, is widely distributed in the mammalian peripheral nervous system and exerts its biological effects mainly by activating the tachykinin NK-2 receptor.[1] Human NK-2 receptor antagonists are considered potential candidates for the treatment of asthma, bronchial hyperreactivity, irritable bowel syndrome, and cystitis.[2] Our studies identified MEN10627 as one of the most potent antagonists for the tachykinin NK-2 receptor, but its very low water solubility did not allow clinical development. The glycosylated derivative nepadutant[3] (cyclo{[Asn(β -D-GlcNAc)-Asp-Trp-Phe-Dap-Leu]cyclo(2β-5β)}) (Figure 1) represents a great improvement in bioavailability, besides being metabolically very stable, and is presently undergoing phase II clinical trials. We have recently shown[4] how a first step in simplifying the structure of nepadutant was undertaken with the discovery of a new series of monocyclic pseudopeptide derivatives. This represented part of a two-branched program: extensive site-directed NK-2 receptor mutagenesis and rationally driven chemical syntheses. The first branch had the aim of identifying and describing the binding site of our reference antagonist (nepadutant) and its chemical evolution derivatives in addition to comparing this binding site with those of other known antagonists; part of this work has already been published.[5] The second branch of the project had the objective to reduce the structural complexity of nepadutant and improve its receptor affinity through the rational design of novel compounds.
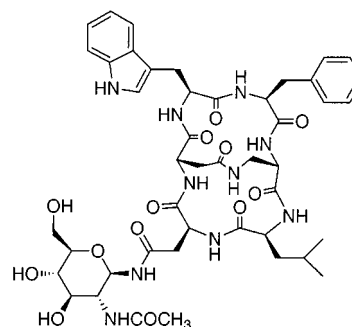

Figure 1. Structure of nepadutant.

This paper reports the complete mutagenesis study, the evolution of a new antagonist series, and the development of a QSAR model with excellent predictive ability.

Site-Directed Mutagenesis

Our previous study[5] considered the residues Gln166, Ser170, Thr171, His198, Tyr206, Tyr266, His267, Phe270, and Tyr289 which are considered to be in the seven transmembrane helices (TM1—7) of the human tachykinin NK-2 receptor. We were able to describe part of the binding site of the peptide NK-2 antagonist nepadutant. The results indicated that Thr171, Tyr206, Tyr266, and Phe270 were involved in the binding of nepadutant, whose binding site was only partially shared with the nonpeptide antagonist SR48968.[6] The two antagonists show significantly different binding modes. The residues to be mutated were selected on the basis of a three-dimensional receptor model which was started from the available knowledge about the relevance of some corresponding residues in the NK-1 receptor. Because of the high level of sequence homology
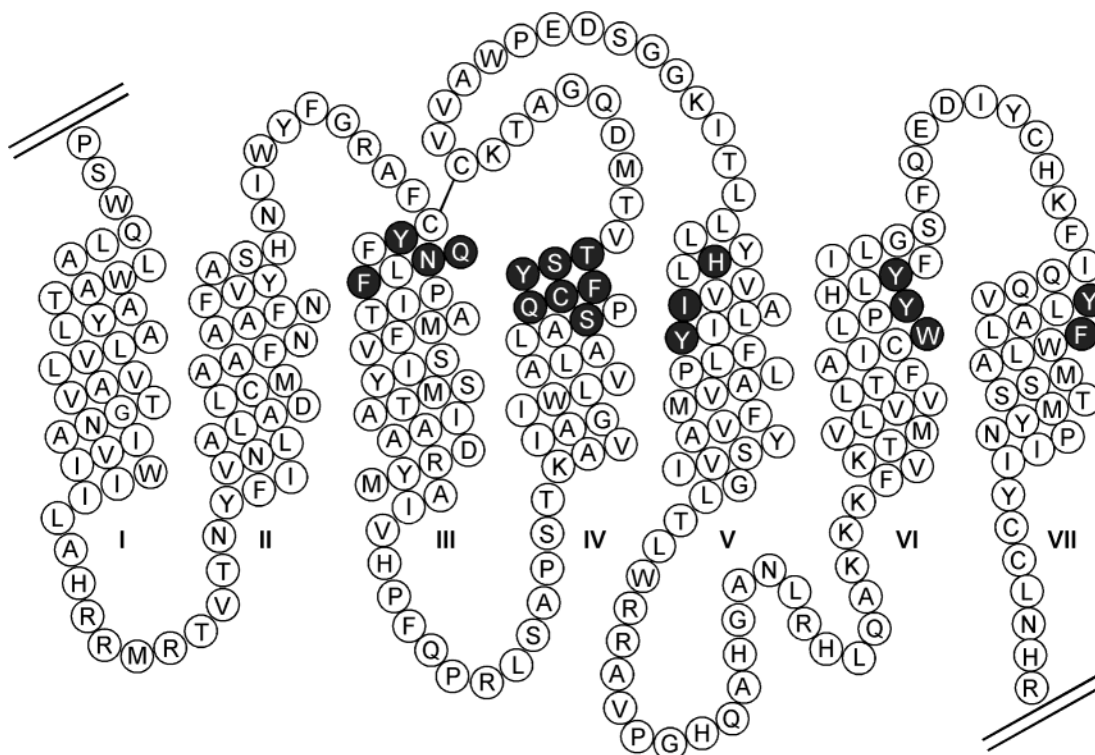
* To whom correspondence should be addressed. Tel: +39 055 5680240. Fax: +39 055 5680241. E-mail: agiolitti@menarini-ricerche.it.
† Department of Drug Design.
‡ Department of Chemistry.
§ Department of Pharmacology.
‖ Department of Biotechnology.

Figure 2. Snake plot of the human NK-2 receptor, updated according to ref 7. Residues indicated with white letters on dark gray circles are those mutated in this work.

and evidence for cross talking between these receptors, some of the conserved residues represented a reasonable starting point. In respect to the previously built model, a new one has been obtained based on the now available crystal structure of bovine rhodopsin.[7] The relative position of the residues in which we were interested was not changed significantly, and we did not have to modify our previous results. The new arrangement is shown in Figure 2. However, a new series of point mutations was necessary to gain a better understanding of the SAR in our peptidic NK-2 antagonists and collect some hints about structural modifications aimed at simplifying nepadutant.

The new point mutations concern Tyr107, Gln109, Asn110, and Phe112 on TM3; Ser164, Cys167, Phe168, and Tyr169 on TM4; Ile202 on TM5; Trp263 and Tyr269 on TM6; and Phe293 on TM7. Data are reported in Table 1.

Monocyclic Antagonists

In the preliminary work,[4] we took a step back from the bicyclic structure of MEN10627,[8] the precursor of nepadutant, to identify the smallest structural subset retaining micromolar affinity for the human NK-2 receptor. This is represented in Figure 3.

The conformational equivalence of the common subset was confirmed.[4] An additional benzyl group was then introduced in different positions of **5a**. The result was MEN11558 (compound **14c** in ref 4) with a pK_i value of 8.7.

MEN11558 (Figure 4) was chosen as the lead compound of this new series of promising NK-2 receptor antagonists. Here, only a small subset of this class of antagonists will be presented, as it is instrumental to

describe the development of a predictive QSAR model. The complete synthetic work will be presented elsewhere.

Structure−Activity Relationships Model

Three-dimensional QSAR methods, such as CoMFA[9] and related techniques, have been proven to be successful tools for correlating structural features with a given biological activity and for predicting the activity of untested compounds.[10] A limitation of these methods is represented by the need to select a conformer (or more than one) for each compound from a conformational analysis which is assigned the label of "bioactive conformation". It is then necessary to define an alignment rule to properly superimpose the compounds to each other and, finally, perform the SAR analysis to build the model.

In the past few years, a QSAR method has been described, termed HQSAR (Hologram QSAR),[11] which is based on fragment fingerprints (a list of all the fragments of a specific length that can be found in a given structure) and their frequency (molecular holograms). Methods such as HQSAR can also produce very good models, as we show here, with a much faster procedure than, for instance, CoMFA, and they are suitable even for the "virtual screening" of large databases. The trade-off is that at the end no real hints are given by the model itself about the best structural direction the synthetic work should take, because no field contour plot is produced like in CoMFA, and the statistical variables in the method have no immediate physical meaning. Fingerprints represent the variables for predicting the biological activity of the corresponding compounds, without the need of selecting a suitable conformer, and properly align each structure. This

Table 1. Binding Affinity Values (means ± sem, n ≥ 3) Determined by Cold Saturation Experiments (to determine K_D) or By Heterologous Competition Experiments (to determine K_i)[a]

hNK-2R		[3H]nepadutant K_D/K_i (nM)						[125I][NKA K_D/K_i (nM)						[3H]SR48968 K_D/K_i (nM)			
		nepadutant	mut/wt	MEN11558	mut/wt	NKA	mut/wt	nepadutant	mut/wt	MEN11558	mut/wt	SR48968	mut/wt	nepadutant	mut/wt	MEN11558	mut/wt
wild type		4.0 ± 0.3	1	4.4 ± 0.8	1	2.4 ± 0.25	1	2.6 ± 0.3	1	2.5 ± 0.7	1	0.6 ± 0.2	1	9.1 ± 3.9	1	14.1 ± 3.2	1
Y107A	TM3	0.75 ± 0.06	0.2	13.6 ± 0.3	3.1	0.5 ± 0.3	0.2										
Q109A	TM3	0.85 ± 0.06	0.2	6.8 ± 0.5	1.5	3.2 ± 1.2	1.3										
N110A	TM3	UB[c]				UB						UB					
F112A	TM3	22.1 ± 7.8	5.5	0.8 ± 0.2	0.2	10.7 ± 0.8	4.3										
S164A	TM4	2.6 ± 0.26	0.6	3.6 ± 0.9	0.8	2.5 ± 0.09	1										
Q166A	TM4	3.5 ± 0.38[b]	0.9	23 ± 0.5	5	6.6 ± 1.3[b]	2.6										
C167A	TM4	UB				UB						0.44 ± 0.2	0.7	>10000	>700	>10000	>700
F168A	TM4	4.1 ± 0.1	1	5.2 ± 0.45	1.2	2.3 ± 0.8	0.9										
Y169A	TM4	4.1 ± 0.9	1	6.5 ± 0.9	1.5	UB											
S170A	TM4	1.5 ± 0.2[b]	0.4	3.5 ± 0.2	0.8	1.9 ± 0.3[b]	0.8	4.5 ± 0.6	1.7	0.76 ± 0.35	0.3						
T171A	TM4	UB[b]				5.9 ± 1.4[b]	2.4										
H198A	TM5	11.5 ± 2.1[b]	2.9	80 ± 41	18	UB[b]											
I202F	TM5	0.44 ± 0.03	0.1	1.6 ± 0.5	0.4	2.1 ± 0.6	0.8										
Y206F	TM5	1.1 ± 0.19[b]	0.3	5.8 ± 0.8	1.3	5.9 ± 1.3[b]	2.4										
W263A	TM6	UB				UB		16.3 ± 3.2	6.3	34 ± 5	13.6	1.2 ± 0.6	2	502 ± 198	55	1070 ± 263	75
Y266F	TM6	UB[b]		UB[b]		2.8 ± 0.2[b]	1.1										
Y269F	TM6	1.7 ± 0.5	0.4	5.9 ± 0.7	1.3	5.3 ± 1.4	2.1										
Y269A	TM6	19 ± 13	4.7	10.1 ± 2.0	2.3	UB											
Y289F	TM7	2.9 ± 0.3[b]	0.7	6.9 ± 2.2	1.6	2.0 ± 0.3[b]	0.8										
Y289T	TM7	11.2 ± 4.3[b]	2.8	19.9 ± 0.09	4.5	UB[b]											
F293A	TM7	7.4 ± 1.2	1.8	12.6 ± 2.3	2.9	40.0 ± 2.4	16										

[a] Affinity changes are expressed as ratios of the corresponding values mutant/wild type (mut/wt). Values >1 represent decreases in affinity, and values <1 represent increases in affinity. Affinity changes statistically significant (underlined) were evaluated according to the 95% confidence limits (P > 0.05) of the respective value and compared with the wild type. [b] See ref 5. [c] Undetectable binding (UB).

MEN10627   5a in Ref. 4
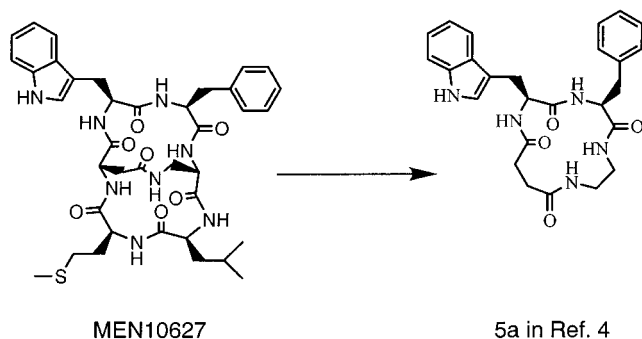
Figure 3. Smallest structural subset in MEN10627 retaining micromolar affinity (from ref 4).
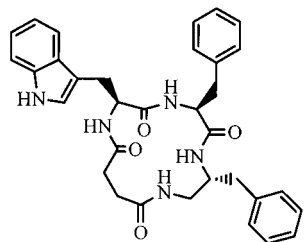
Figure 4. Structure of MEN11558.

allows a rapid obtainment of good QSAR models, even from large sets of molecules; such models can be used by the bench chemist to check proposed modifications and to put them in rank order in terms of synthetic priority.

Table 2 reports the compounds used in the training set and their pK_i values as produced by the HQSAR models and experimental methods.

Results

Site-Directed Mutagenesis. A total of 21 mutant human NK-2 receptors were studied to define the binding site of the reference compound MEN11558, especially in respect to the binding site of nepadutant. These results and those concerning the behavior of MEN11558 on mutants previously tested against nepadutant[5] are reported in Table 1. When the mutations did not allow an evaluation of the binding of [3H]nepadutant, the affinities of nepadutant and MEN11558 were tested against [125I]NKA. Here, a comment is outlined for each significant mutation.

Tyr107Ala. It negatively affects the binding of MEN11558 by 3-fold reduction but not that of nepadutant.

Asn110Ala. None of the radioligands we tested exhibited binding affinity for this mutant; this suggests a significant modification in either overall receptor conformation (tertiary structure) or receptor expression.

Phe112Ala. The binding of nepadutant and NKA is decreased by approximately 5- and 4-fold, respectively.

Gln166Ala. This mutation was previously reported not to affect the binding of nepadutant;[4] on the other hand, the affinity of MEN11558 is decreased 5-fold.

Cys167Gly. A relevant effect is produced by this substitution which completely abolishes the binding of nepadutant. Gly is the residue in the hNK-1 receptor which corresponds to Cys167 in the hNK-2 receptor. This mutation also abolishes the binding of NKA which, on the other hand, binds, albeit with lower affinity, the

NK-1 receptor.[12] This appears to support the hypothesis that NKA binds differently to the NK-2 and NK-1 receptors. In agreement with the lack of binding by [3H]nepadutant radioligand, competition binding experiments, with respect to the nonpeptide antagonist [3H]SR48968, confirmed the drastic loss of affinity by both nepadutant and MEN11558.

Tyr169Ala. While abolishing the binding of NKA, this mutation does not impair the binding of nepadutant and MEN11558. Therefore, it appears to be a residue relevant to the binding of the natural agonist.

Thr171Ala. No determination of a K_D value was possible by direct binding of [3H]nepadutant. Against [125I]NKA, both nepadutant and MEN11558 maintained their affinity.

His198Ala. The mutation impairs the binding of MEN11558 18-fold, even more than that of nepadutant, in addition to drastically preventing the binding of the natural agonist.

Ile202Phe. This residue was mutated to Phe as it is in mouse, rat, and hamster NK-2 receptors. The mutation increases the binding of nepadutant by about 1 order of magnitude but not that of NKA. This result is in agreement with the functional data we previously obtained from the human and mouse NK-2 receptors; the apparent affinity of nepadutant, determined as pK_B, in blocking the contractile effect produced by the agonist NKA was significantly higher at the mouse (pK_B 9.8[3]) NK-2 receptors than at the human (pK_B 8.5[13]) NK-2 receptors, as expressed in urinary bladder preparations.

Trp263Ala. No binding could be detected for [3H]nepadutant and [125I]NKA; therefore, [3H]SR48968 was evaluated. This nonpeptide ligand maintained an affinity value comparable to that observed with the wild type, while both nepadutant and MEN11558 had their binding strongly impaired (55- and 75-fold, respectively).

Tyr266Phe. As in the case of Thr171Ala, [125I]NKA had to be used as a radioligand, but with this mutant, both nepadutant and MEN11558 had their affinity decreased (6- and 13-fold, respectively).

Tyr269Ala and -Phe. We have shown[5] that Tyr266, which is located about one helical turn above Tyr269, is part of the binding site of nepadutant. Tyr269, especially with its phenyl ring, affects the binding of nepadutant and MEN11558 (5- and 2-fold, respectively).

As suggested previously,[4] nepadutant and MEN11558 share most of their binding sites; here, we show different binding behavior at Tyr107, Phe112, and Gln166 which are located on TM3 and TM4. This is in agreement with our proposed model[4,5] and the structural differences between the two compounds.

Modeling and QSAR. The first series of 25 compounds, reported in rows 1−25 in Table 2, was examined using the HQSAR module in Sybyl (Tripos Inc., St. Louis, MO). The corresponding results are reported in Table 2 as MOD1. The standard error in prediction (SE of Q^2) is quite high; with the evaluation of the absolute differences between the experimental pK_i and cross-validated (predicted) values (CV), one of the compounds, MEN11690, showed a gap of 2 log units (exp, 10.0; CV predicted, 7.99). Compound competition curves of [125I]NKA displayed a shallow slope (significantly less than unity) fitting a two-site model with the two K_i values calculated as 3 and 1.2 nM, respectively. The

Table 2. Structures of the 29 Compounds Used To Develop the Initial HQSAR Models MODn[a]

		pK$_i$						
MEN	Structure	Exp.	MOD1	MOD2	MOD3	MOD4	MOD4 pred	MOD5
11523		5.4	5.8	5.9	5.9	5.7	5.4	
11532		6.2	6.2	6.2	6.1	6.1	6.1	
11540		6.1	6.3	6.4	6.3	6.4	6.2	
11558		8.7	8.4	8.1	8.1	8.2	8.3	
11667		6.5	7.1	7.0	7.0	7.1	6.5	
11668		7.9	8.6	8.3	8.4	8.3	8.4	
11690		10.0	8.0	-	-	-	-	
11691		8.5	8.6	8.3	8.4	8.3	8.4	8

Table 2 (Continued)
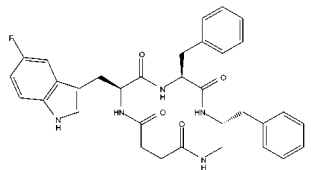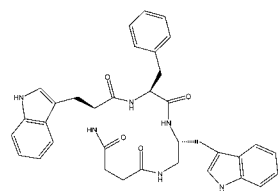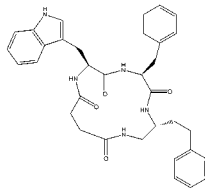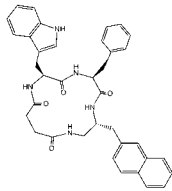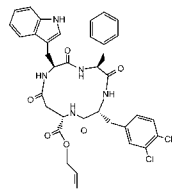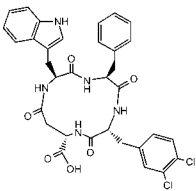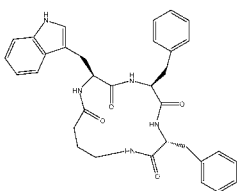
MEN	Structure	pK$_i$						
		Exp.	MOD1	MOD2	MOD3	MOD4	MOD4 pred	MOD5
11701		8.5	8.5	8.3	8.3	8.4	8.5	8
11703		8.5	7.7	7.6	7.7	7.7	8.6	8
11708		8.0	7.8	7.9	7.9	8.1	8.2	8
11712		8.1	8.1	8.4	8.3	8.2	8.1	8
11715		6.5	6.8	6.3	6.3	6.4	6.4	6
11716		6.4	6.8	6.4	6.5	6.6	6.4	6
11733		6.5	6.8	6.8	6.8	6.9	6.5	6.5

Table 2 (Continued)
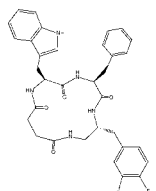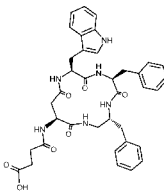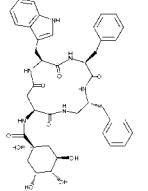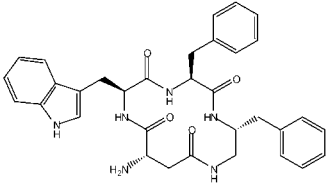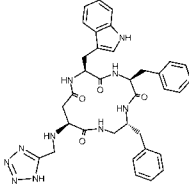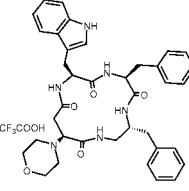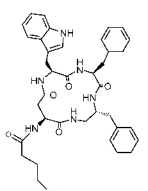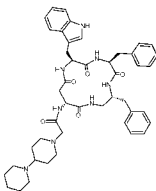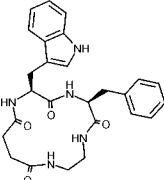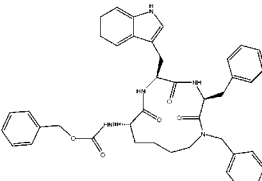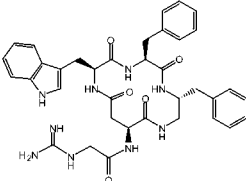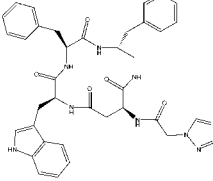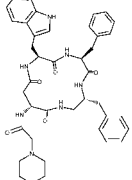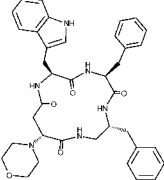
MEN	Structure	pK$_i$					MOD4 pred	MOD5
		Exp.	MOD1	MOD2	MOD3	MOD4		
11749		8.8	8.6	8.6	8.6	8.7	8.9	8.6
11755		7.9	8.4	8.4	8.3	8.2	7.9	8.3
11757		8.2	8.8	8.2	8.0	8.7	8.3	8.3
11799		8.5	8.5	8.3	8.4	8.5	8.6	8.6
11830		8.8	8.9	8.8	8.9	8.7	8.7	8.6
11842		9.1	9.0	8.8	9.9	9.5	9.2	9.3
11877		8.1	8.2	8.3	8.2	8.1	8.0	8.2
11959		9.4	8.9	8.9	9.2	9.3	9.4	9.2

Table 2 (Continued)

| MEN | Structure | pK$_i$ | | | | | | |
		Exp.	MOD1	MOD2	MOD3	MOD4	MOD4 pred	MOD5
11970		5.9	6.0	5.7	5.7	5.9	6.0	6.0
11983		8.3	7.1	8.0	8.1	8.0	8.3	8.5
11986		8.4	-	(8.4)	8.3	8.4	8.4	8.4
11987		8.4	-	(8.6)	8.6	8.4	8.4	8.6
11990		9.5	-	(8.7)	8.8	9.2	9.5	9.4
11995		9.8	-	(9.1)	9.4	9.3	9.7	9.8

[a] Numbers in each MOD*n* column are predicted pK$_i$ values in cross-validated mode, except for the "MOD4 pred" column. Numbers in the MOD5 column refer to the values predicted (cross-validated mode) by the final model for these compounds. Values in brackets in column "MOD2" for the last four compounds are those predicted by model 2 before the compounds were included in model 3.

resulting mean pK$_i$ value is higher than that corresponding to the common binding site only. Therefore, this compound was excluded from the training set, as its value could not properly be explained in a simple way by the model.

The new model is MOD2 with 24 rows in Table 3. While Q^2 is slightly worse, R^2 and the standard error improved, even if the corresponding standard error is lower. This model was used to predict the binding values of four new compounds (rows 26−29 in Table 2) with the following results: MEN11986 = 8.3 (exp, 8.4),

MEN11987 = 8.4 (exp, 8.4), MEN11990 = 8.7 (exp, 9.5), and MEN11995 = 9.2 (exp, 9.8).

A new model was calculated including these 28 compounds, with the results reported as MOD3 in Table 2. This model was also tested for chance correlation using a randomization routine which confirmed the quality of the result. A parameter was then modified to take chirality into account. With the option "chirality ON" in HQSAR, the model resulted in MOD4 in Table 2. Since then, the HQSAR model has progressed to the present MOD5 (Tables 2 and 3) which includes 313

Table 3

model	no. compd	R^2 (SE)	Q^2 (SE)	compd	options[a]
1	25	0.95 (0.29)	0.77 (0.64)	3	A,B,C: ON H,Ch,DA: OFF Atm in Fr.: 4–7
2	24	0.98 (0.19)	0.75 (0.62)	4	A,B,C: ON H,Ch,DA: OFF Atm in Fr.: 4–7
3	28	0.98 (0.19)	0.90 (0.42)	5	A,B,C: ON H,Ch,DA: OFF Atm in Fr.: 4–7
4	28	0.99 (0.12)	0.91 (0.40)	6	A,B,C,Ch: ON H,DA: OFF Atm in Fr.: 4–7
5	313	0.88 (0.44)	0.86 (0.49)	6	A,B,C,Ch: ON H,DA: OFF Atm in Fr.: 4–7

[a] Options in HQSAR model building: A, atoms; B, bonds; C, connections; H, hydrogens; Ch, chirality; DA, donor & acceptor.

compounds. While statistics for this model are clearly weaker than those for the previous MOD4, MOD5 is able to accommodate a greater variability in functional groups and shows excellent stability by being able to include and predict different classes of compounds (data not shown).

Discussion

Results from site-directed mutagenesis studies allowed us to hypothesize a binding site for the representative of the new series of antagonists, namely, MEN11558, which are largely superimposable to that of nepadutant. The residues significantly affecting the binding of nepadutant and MEN11558 are Cys167 in TM4, His198 in TM5, and Trp263, Tyr266, and Tyr269 in TM6. Gln166, on the other hand, seems to interact with MEN11558 but not with nepadutant. These residues are proposed to interact with the common structural features of the two antagonists, although there is no clear evidence, among the residues we mutated, of

interactions discriminating between the two. However, since the binding site appears to be proximal to the extracellular site of the receptor, we can suppose that the glycosidic moiety of nepadutant could interact with more polar loop residues. This is shown in Figures 3 and 4. Figure 5 shows a proposed binding mode for MEN11558 with the relevant receptor residues evident. It should be mentioned again that the models are still speculative, because there is no crystal structure available for these complexes. However, we could maintain the starting hypotheses about the main structural features of the monocyclic compounds, as derived from our knowledge of the nepadutant series. Different binding behavior is found, as expected, for mutations in the residues belonging to TM3 and TM4 which, in our model, correspond to the nonconserved part of the ligand structure. Since the mutant receptors are stably transfected, they are usefully employed to check structural modifications in the monocyclic antagonist series.

As we said before, we cannot deduce the nature of the molecular interactions, that is, which part of the ligand interacts with which part of the receptor, from HQSAR models directly. However, the binding modes suggested even by the manual docking of the ligands in receptor models[14] on the basis of mutagenesis data can be a very useful guide for selecting new ligand moieties and substituents. The HQSAR model, on the other hand, is an efficient tool for helping assign priorities to the proposed chemical syntheses, as it is very fast in checking new structures, because it does not require the assignment of a "bioactive conformation" or an alignment rule. It is not efficient, however, in proposing structural modifications favorable for activity, which rely on the knowledge and intuition of the medicinal chemists. For instance, it is clear that a proper amino group and a hydrogen bond acceptor close to it have a favorable effect on the binding to the receptor (see, for instance, the amino side chain in MEN11995). On the
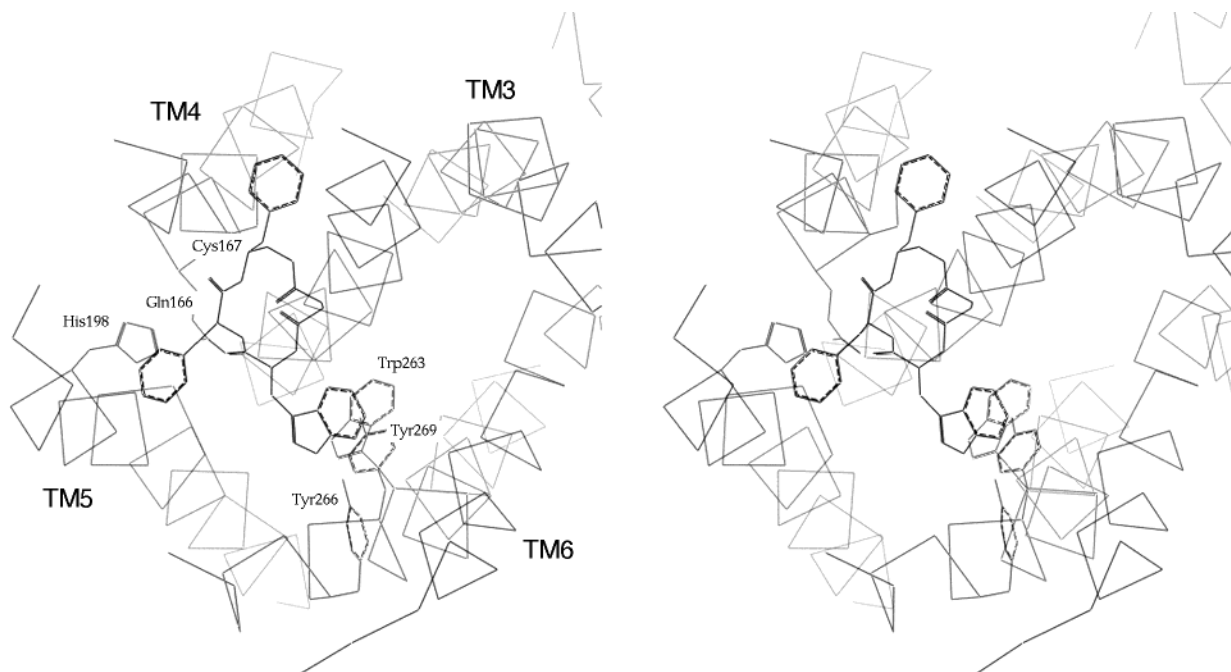
Figure 5. Cα trace of the three-dimensional receptor model (stereoview, TM only), as viewed from the extracellular side, reporting the hypothesis for nepadutant binding mode on the human NK-2 receptor as reported in ref 5.

other hand, there are no good candidates among the residues in the receptor model for such an interaction once the ligand has been docked. We suspect, therefore, that the basic moiety of the ligands interacts with the residues belonging to the extracellular loops of the receptor which lie on top of the transmembrane helices, as suggested by the crystal structure of bovine rhodopsin.[7] Since these are usually not conserved among GPCRs and depend strongly on the specific receptor, they are not properly modeled and, therefore, are generally left out from the receptor model itself, as in this case.

In conclusion, the aim of this program was two-fold: (1) to describe in molecular terms the binding site of our pseudopeptide hNK-2 receptor antagonists, correlate ligand structural features to specific residues in the receptor, and define how much of the available knowledge gained from the bicyclic antagonists, such as nepadutant, could be transferred to the new simplified series; and (2) to develop a QSAR working tool to support the synthetic effort toward smaller and more active antagonists.

Experimental Section

(A) Compound Syntheses. Compounds **2**−**7**, **11**, **12**, **16**, and **24** in Table 2 were synthesized as in ref 4. The compounds **8**−**10**, **17**−**22**, and **29** were synthesized as in Patent WO 9834949, and compounds **26**−**28** were synthesized as in Patent WO 0008046. The other compounds were obtained as follows.

General Methods. ^{1}H-NMR spectra were acquired at 500 MHz on a Bruker Advance spectrometer. Mass spectra were acquired by positive-ion electrospray ionization (ES) on a Finnigan LCQ ion trap mass spectrometer, introducing the sample by infusion via a built-in syringe pump. Melting points were determined using a Büchi melting point apparatus and were not corrected. Preparative HPLC was performed on a Shimadzu LC-10 apparatus. The following abbreviations are used for the reagents and solvents: All, allyl; Boc, *tert*-butyloxycarbonyl; dba, dibenzylideneacetone; DIPEA, *N,N*-diisopropylethylamine; DMF, *N,N*-dimethylformamide; DMSO, dimethyl sulfoxide; Dpr, (*S*)-2,3-diaminopropionic acid; EDC, 1-ethyl-3-(3-dimethylaminopropyl)carbodiimide hydrochloride; Fmoc, (9-fluorenyl-methoxy)carbonyl; HOBt, 1-hydroxybenzotriazole; Phe, (*S*)-phenylalanine; PyBOP, (benzotriazol-1-yloxy)-tripyrrolidinophosphonium hexafluorophosphate; TEA, triethylamine; TFA, trifluoroacetic acid; THF, tetrahydrofuran; Trp, (*S*)-tryptophan; and Z, benzyloxycarbonyl.

6-(*S*)-Benzyl-9-(*S*)-(1*H*-indol-3-ylmethyl)-5,8,11,14-tetraoxo-1,4,7,10-tetraaza-cyclotetradecane-3-(*S*)-carboxylic Acid Amide (1). To a solution of Boc-Trp-Phe-OH (1.20 g, 2.66 mmol) in dichloromethane (10 mL) were added H-Dpr(Z)-NH₂·TFA (0.95 g, 2.7 mmol) and PyBOP (1.70 g, 3.27 mmol) in sequence under a nitrogen atmosphere. After the mixture was stirred for 10 min, TEA (1.48 mL, 10.6 mmol) was added, and the resulting solution was stirred overnight. Evaporation of the solvent gave a residue that was purified by flash chromatography (silica gel, ethyl acetate) giving 0.95 g (1.42 mmol, 53% yield) of Boc-Trp-Phe-Dpr(Z)-NH₂ as a white solid. The compound was suspended in dichloromethane (45 mL), and TFA (5 mL, 64.9 mol) was added; the solution was stirred for 90 min and evaporated. After the mixutre was dried in vacuo for 24 h, 787 mg (1.38 mmol, 97% yield) of H-Trp-Phe-Dpr(Z)-NH₂ was obtained. The compound was dissolved in anhydrous DMF (20 mL) under a nitrogen atmosphere. Succinic anhydride (166 mg, 1.66 mmol) and DIPEA (0.29 mL, 1.66 mmol) were added, and the solution was stirred for 2 h. After evaporation under reduced pressure, the residue was treated with water (8 mL), and the obtained white solid was filtered off, washed on the filter with water (2 × 8 mL), and dried giving 760 mg (1.13 mmol, 82% yield) of *N*-[1-[1-(2-benzyloxy-carbonylamino-1-(*S*)-carbamoyl-ethylcarbamoyl)-2-(*S*)-phenyl-

ethylcarbamoyl]-2-(*S*)-(1*H*-indol-3-yl)-ethyl]-succinamic acid. The compound was suspended in anhydrous ethanol (150 mL), and 10% Pd/C (450 mg) was added; the mixture was maintained under a hydrogen flow for 4 h. After being filtered and washed with ethanol (2 × 30 mL), the solution was evaporated giving *N*-[1-[1-(2-amino-1-(*S*)-carbamoyl-ethylcarbamoyl)-2-(*S*)-phenyl-ethylcarbamoyl]-2-(*S*)-(1*H*-indol-3-yl)-ethyl]-succinamic acid (499 mg, 0.93 mmol, 82% yield). The compound was dissolved in anhydrous DMF (75 mL) under a nitrogen atmosphere; PyBOP (600 mg, 1.11 mmol) and DIPEA (0.58 mL, 3.34 mmol) were added, and the solution was stirred for 2 h at room temperature. After evaporation in vacuo, the residue was purified by reverse phase flash chromatography (Matrex C18, 60 Å pore diameter, 50 mm particle size; mobile phase: acetonitrile/water, 50:50 v/v) giving 154 mg (0.30 mmol, 32% yield) of **1**: ^{1}H-NMR (DMSO-d_6, ∂) 2.15−2.35 (2H, m), 2.55−2.85 (8H, m), 3.60−3.72 (1H, m), 3.95−4.18 (1H, m), 4.25−4.42 (1H, m), 6.71 (1H, d, $J = 9$ Hz), 6.90−7.40 (9H, m), 7.43 (1H, d, $J = 8$ Hz), 8.09 (1H, m), 8.50 (1H, d, $J = 6$ Hz), 10.82 (1H, br s); MS (ES⁺) m/z 519 (MH⁺).

5(*S*)-Benzyl-8(*R*)-(3,4-dichloro-benzyl)-2(*S*)-(1*H*-indol-3-ylmethyl)-3,6,9,14-tetraoxo-1,4,7,10-tetraaza-cyclotetradecane-11-carboxylic Acid Allyl Ester (13). H-Trp-Phe-OtBu (580 mg, 1.42 mmol) and Fmoc-Asp(OH)-OAll (570 mg, 1.42 mmol) were dissolved in DMF (30 mL). EDC (280 mg, 1.46 mmol) and HOBT (767 mg, 5.67 mmol) were added, and the solution was stirred overnight at room temperature. After evaporation of the solvent, water (150 mL) was added to the residue, giving a white solid that was filtered and dissolved in ethyl acetate (50 mL). The organic phase was washed with 10% aqueous (aq) citric acid (2 × 30 mL); it was then washed with 5% aq NaHCO₃ (2 × 30 mL), and then with water (30 mL). After the solution was dried over Na₂SO₄ and evaporated under reduced pressure, the residue was purified by flash chromatography (ethyl acetate/cyclohexane, 50:50 v/v), giving 800 mg (73% yield) of 4-[1-(1-*tert*-butoxycarbonyl-2(*S*)-phenyl-ethylcarbamoyl)-2(*S*)-(1*H*-indol-3-yl)-ethylcarbamoyl]-2-(2-9*H*-fluoren-9-yl-oxycarbonylamino)-butyric acid allyl ester. The residue was dissolved in anhydrous THF (25 mL), and the Fmoc group was removed by stirring the solution for 90 min with excess diethylamine (2.5 mL, 24 mmol). After the solvent was evaporated, the residue was purified by flash chromatography (ethyl acetate/methanol, 95:5 v/v), giving 430 mg (82% yield) of 2-amino-4-[1-(1-*tert*-butoxycarbonyl-2(*S*)-phenyl-ethylcarbamoyl)-2(*S*)-(1*H*-indol-3-yl)-ethylcarbamoyl]-butyric acid allyl ester. The compound was dissolved in anhydrous DMF (20 mL) together with 256 mg (0.77 mmol) of *N*-Boc-3,4-dichlorophenylalanine. EDC (154 mg, 0.80 mmol) and HOBt (311 mg, 2.3 mmol) were added in sequence, and the mixture was stirred for 20 h at room temperature. After the solvent was concentrated to a small volume, the residue was diluted with water (30 mL), giving a white solid that was dissolved in ethyl acetate (30 mL). The organic phase was separated and washed with 10% aq citric acid (2 × 20 mL); it was then washed with 5% aq NaHCO₃ (2 × 20 mL), and then with water (20 mL). After being dried over Na₂SO₄, the separated organic phase was evaporated under reduced pressure to obtain 2-[2-*tert*-butoxycarbonylamino-3(*R*)-(3,4-dichloro-phenyl)-propionylamino]-4-[1-(1-*tert*-butoxycarbonyl-2(*S*)-phenyl-ethylcarbamoyl)-2(*S*)-(1*H*-indol-3-yl)-ethylcarbamoyl]-butyric acid allyl ester as a yellowish solid (657 mg, 97% yield). The *N*-Boc protecting group and the *tert*-butyl ester were removed by treatment with TFA (10 mL, 0.13 mol) and methyl sulfide (70 µL, 1.6 mmol) for 30 min at room temperature. After the evaporation of TFA, the crude residue (white solid, 500 mg, 96% yield) was dissolved in anhydrous DMF. TEA (96 µL, 0.69 mmol) was added followed by EDC (135 mg, 0.7 mmol) and HOBt (281 mg, 2.07 mmol). The solution was stirred overnight at room temperature and evaporated to give a yellow oil. The addition of water gave a yellowish solid that was filtered out and dissolved in ethyl acetate (30 mL). The organic phase was washed with 5% aq KHSO₄ (20 mL); it was then washed with 10% aq NaHCO₃ (20 mL), and then with water (2 × 20 mL). After the solution was dried over Na₂SO₄ and

the solvent evaporated under reduced pressure, **13** was obtained as a white solid (335 mg, 0.48 mmol, 34% overall yield): ^{1}H-NMR (DMSO-d_6, ∂) 2.53 (2H, m), 2.63 (2H, ABq, J = 5, 14 Hz), 4.30 (1H, m), 4.31 (1H, m), 4.37 (1H, m), 4.57 (2H, m), 4.71 (1H, m), 5.19 (1H, m), 5.32 (1H, m), 5.89 (1H, m), 6.97 (1H, m), 7.67 (1H, d, J = 8.6 Hz), 7.94 (1H, d, J = 8.3 Hz), 8.77 (1H, d, J = 8.5 Hz), 10.87 (1H, d, J = 2.2 Hz); MS (ES[+]) m/z 704 (MH[+]).

5(S)-Benzyl-8(R)-(3,4-dichloro-benzyl)-2(S)-(1H-indol-3-ylmethyl)-3,6,9,14-tetraoxo-1,4,7,10-tetraaza-cyclotetradecane-11-carboxylic Acid Allyl Ester (14). Compound **13** (150 mg, 0.21 mmol) was dissolved under a nitrogen atmosphere in anhydrous THF (30 mL). Pd(dba)$_2$ (126 mg, 0.22 mmol) was added, followed by triphenylphosphine (82 mg, 0.31 mol) and acetic acid (18 μL, 0.31 mmol). After the mixture was stirred for 1 h at room temperature, the solvent was evaporated under reduced pressure giving a greenish residue. Diethyl ether (10 mL) was added, and the solid residue was filtered under a nitrogen atmosphere, washed several times on the filter with diethyl ether, and dried. Purification by reverse phase flash chromatography (Matrex C18, 60 Å pore diameter, 50 μm particle size; mobile phase: acetonitrile/water, 50:50 v/v) gave 70 mg (0.105 mmol, 50% yield) of **14** as a white solid: mp 290−305 °C dec; ^{1}H-NMR (DMSO-d_6, ∂) 2.53 (2H, m), 2.64 (2H, ABq, J = 5, 14 Hz), 4.29 (1H, m), 4.36 (1H, m), 4.52 (1H, m), 7.64 (1H, m), 7.94 (1H, m), 8.76 (1H, d, J = 8.5 Hz), 10.86 (1H, d, J = 2.2 Hz); MS (ES[+]) m/z 664 (MH[+]).

(3S,6R)-Dibenzyl-9-(S)-(1H-indol-3-ylmethyl)-1,4,7,10-tetraaza-cyclotetradecane-2,5,8,11-tetraone (15). N-Boc-4-aminobutyric acid (500 mg, 2.46 mmol) was dissolved in 25 mL of anhydrous DMF. EDC (480 mg, 2.50 mmol), HOBt (1.0 g, 6.5 mmol), and H-Trp-Phe-OtBu (1.0 g, 2.45 mmol) were added in sequence, and the resulting solution was stirred overnight at room temperature. After the solution was concentrated to a small volume, the residue was diluted with ethyl acetate. The organic phase was washed with 10% aq citric acid; it was then washed with 5% aq sodium bicarbonate, and finally with water. After the mixture was dried over Na$_2$SO$_4$, evaporation under reduced pressure gave (2R)-{2-(S)-[2-(4-$tert$-butoxycarbonylamino-butyrylamino)-3-(S)-(1H-indol-3-yl)-pro-pionylamino]-3-phenyl-propionylamino}-3-phenyl-propionic acid $tert$-butyl ester as a yellowish solid (1.27 g, 2.40 mmol, 98% yield). The crude product was dissolved in dichloromethane (20 mL), and the solution was cooled to 0 °C. TFA (4.25 mL, 55 mmol) was added dropwise. The resulting solution was allowed to warm to room temperature and was stirred for 1 h. After evaporation of the solvent, the addition of water and sodium carbonate gave a white precipitate that was filtered out and dissolved in ethyl acetate. The organic phase was washed with water to a neutral pH. After the mixture was dried over MgSO$_4$ and the solvent evaporated under reduced pressure, (2R)-{2-(S)-[2-(4-amino-butyrylamino)-3-(S)-(1H-indol-3-yl)-propionylamino]-3-phenyl-propionylamino}-3-phenyl-propionic acid $tert$-butyl ester was obtained as a porous white solid (662 mg, 1.34 mmol, 56% yield). The crude product was added to a solution of N-Boc-(R)-phenylalanine (353 mg, 1.34 mmol), EDC (274 mg, 1.42 mmol), and HOBt (542 mg, 4.0 mmol) in anhydrous DMF (40 mL). The mixture was stirred overnight at room temperature, and then evaporated; the residue was dissolved in ethyl acetate and washed with 5% aq KHSO$_4$, 5% aq NaHCO$_3$, and water. After the mixture was dried over MgSO$_4$ and the solvent evaporated under reduced pressure, (2R)-{2-(S)-[2-[4-(2-$tert$-butoxycarbonylamino-3-phenyl-propionylamino)-butyrylamino]-3-(S)-(1H-indol-3-yl)-propionylamino]-3-phenyl-propionylamino}-3-phenyl-propionic acid $tert$-butyl ester was obtained as a white solid (803 mg, 1.08 mmol, 81% yield). The crude product was added to a solution of methyl sulfide (0.26 mL, 3.5 mmol) in 18 mL of TFA, and the mixture was stirred for 1 h at room temperature. After the evaporation of TFA, the crude residue was repeatedly treated with diethyl ether to give a white solid; the white solid was filtered off, dried, and dissolved in 90 mL of anhydrous DMF. After the addition of EDC (210 mg, 1.09 mmol), HOBt (440 mg, 3.25 mmol), and TEA (0.175 mL, 1.25 mmol), the

solution was stirred overnight at room temperature, and then evaporated; the residue was dissolved in ethyl acetate. The organic phase was washed with 5% aq KHSO$_4$, 5% aq NaHCO$_3$, and brine. After the mixture was dried over MgSO$_4$, evaporation of the solvent under reduced pressure gave a yellowish solid. Purification by reverse phase flash chromatography (Matrex C18, 60 Å pore diameter, 50 μm particle size; mobile phase: acetonitrile/water, 50:50 v/v) gave 275 mg (0.486 mmol, 45% yield) of **15** as a white lyophilized solid: ^{1}H-NMR (DMSO-d_6, ∂) 1.45−1.53 (1H, m), 1.87−1.97 (1H, m), 2.21−2.37 (2H, m), 2.56−2.90 (5H, m), 3.22−3.26 (1H, m), 3.28−3.35 (m, partially overlapped with the water signal), 3.58−3.65 (1H, m), 4.07−4.12 and 4.15−4.18 (2H, 2 m), 4.46−4.52 (1H, m), 6.95−7.25 (13, m), 7.33 (1H, d, J = 8 Hz), 7.45 (1H, d, J = 8 Hz), 8.32 (1H, d, J = 5 Hz), 8.51 (1H, d, J = 8 Hz), 10.8 (1H, d, J = 3 Hz); MS (ES[+]) m/z 566 (MH[+]).

2-[1,4′]Bipiperidinyl-1′-yl-N-[(5S,8R)-dibenzyl-2-(S)-(1H-indol-3-ylmethyl)-3,6,11,14-tetraoxo-1,4,7,10-tetraaza-cy-clotetradec-12-(R)-yl]-acetamide (23). To a suspension of 500 mg (2.2 mmol) of [1,4′-bipiperidine]-1′-acetic acid[15] were added, in 30 mL of DMF, HOBt (770 mg, 5.7 mmol) and EDC (360 mg, 1.88 mmol) in sequence. After the mixture was stirred at room temperature for 10 min, 1.11 g (1.91 mmol) of (12R)-amino-(5S,8R)-dibenzyl-2-(S)-(1H-indol-3-ylmethyl)-1,4,7,10-tetraaza-cyclotetradecane-3,6,11,14-tetraone[16] was added, and the solution was stirred for 2 h at the same temperature. Evaporation of the solvent gave a crude residue that was treated with ethyl acetate. The solid precipitate was filtered off and dried, giving a crude product. Purification by reverse phase flash chromatography (Matrex C18, 60 Å pore diameter, 50 mm particle size; mobile phase: acetonitrile/water, 50:50 v/v) gave **23** as a white solid (655 mg, 0.83 mmol, 43% yield): ^{1}H-NMR (DMSO-d_6, ∂) 1.45−1.65 (2H, m), 1.65−1.85 (6H, m), 1.91−2.03 (2H, m), 2.33−2.50 (3H, m), 2.78−2.82 (5H, m), 2.85−3.70 (m, overlapped with the water signal), 4.04−4.09 (1H, m), 4.10−4.14 (1H, m), 4.23−4.35 (1H, m), 4.74−4.80 (1H, m), 6.81−6.69 (1H, d, J = 9 Hz), 6.95−7.40 (12H, m), 7.46 (1H, d, J = 8 Hz), 7.52−7.61 (1H, m), 8.30 (1H, d, J = 9 Hz), 8.50 (1H, d, J = 5 Hz), 10.62 (1H, br s); MS (ES[+]) m/z 789 (MH[+]).

(B) Biology. Radioligand Binding Experiments. Stable transfection of wild type and mutant receptors and membrane preparation were carried out as previously described.[5] The buffer used for binding experiments was Tris-HCl (50 mM, pH 7.4) which contained bacitracin (100 mg mL^{−1}), chymostatin (10 mg mL^{−1}), leupeptin (5 mg mL^{−1}), thiorphan (10 mM), NaCl (150 mM), MnCl$_2$ (5 mM), and bovine serum albumin (1 g L^{−1}). The binding assay was performed in a final volume of 0.5 mL for 30 min ([125I]NKA and [3H]SR48968) or 60 min ([3H]ne-padutant) at 20 °C. [3H]Nepadutant (specific activity, 62 Ci mmol^{−1}) was synthesized by SibTech Inc. (Elmsford, NY). [125I]NKA (specific activity, 2000 Ci mmol^{−1}) and [3H]SR48968 (specific activity, 25 Ci mmol^{−1}) were purchased from Amersham (Buckinghamshire, U.K.) and NEN Life Sciences Products (Boston, MA), respectively. Competition binding experiments were carried out at the agonist and antagonist radioligand concentration below its affinity constant, which bound less than 10% of the total added radioligand. Preliminary experiments were performed to determine membrane protein concentrations (50−300 μg mL^{−1}) of each receptor in order to obtain a signal of 1500−4000 dpm/assay of specific binding. Nonspecific binding was defined as the amount of labeled radioligand bound in the presence of 1 mM appropriate unlabeled ligand, and it represented less than 5% of total bound radioligand. All of the compound competition curves were tested in a wide range of concentrations (0.3 pM to 10 μM). The assay was started by the addition of 0.4 mL of membrane suspension, and it was terminated by the rapid filtration through UniFilter-96 plates (Packard) that had been presoaked for at least 2 h in polyethylenimine (PEI) 0.3%, using a MicroMate 96 Cell Harvester (Packard Instrument Company). The tubes and filters were then washed 5 times with 0.5 mL aliquots of Tris buffer (50 mM, pH 7.4, 4 °C). Filters were dried and soaked in Microscint 40 (Packard Instrument Company), and bound radioactivity was counted

by a TopCount Microplate Scintillation Counter (Packard Instrument Company).

Radioligand binding experiments were analyzed by fitting the data with the GraphPad Prism program (San Diego, CA) for Apple Macintosh in order to determine the −log of the inhibitory affinity constant (pK_i) for heterologous competition experiments and the −log of the radioligand affinity constant (−log K_D) for homologous competition experiments, and were expressed as the mean ± standard error of the mean from the stated number of experiments, each performed in duplicate.

(C) Modeling and QSAR. In the case of our NK-2 antagonists, the model has been built initially from a small set of 24 compounds (Table 2). Newly synthesized compounds have been progressively tested against the available model, and then included in a new recomputed one.

HQSAR parameters were essentially set at their default values, as shown in Table 3, and are reported here. Atom count in fragments: min 4; max 7 (default 3−6). Atoms, bonds, connections: ON. Hydrogen atoms, chirality, donor & acceptor: OFF. Hologram lengths: 53−353. Select best model based on: least standard error. In the last model the "Chirality" flag was ON. Table 3 reports the statistics for these five models. The structures were built in Sybyl 6.4 (Tripos, Inc.) with a careful check of atom types but no conformational search. The parameters in HQSAR were initially set at their default values, and were later adjusted to include chirality and the optimal fragment length of 4−7 atoms (no hydrogens). Q is the cross-validated correlation coefficient derived from the predictive residual sum of squares.

References

(1) Regoli, D.; Boudon, A.; Fauchere, J. Receptors and antagonists for substance P and related peptides. *Pharmacol. Rev.* **1994**, *46* (4), 551−599.

(2) Maggi, C. A.; Patacchini, R.; Rovero, P.; Giachetti, A. Tachykinin receptors and tachykinin receptor antagonists. *J. Auton. Pharmacol.* **1993**, *13*, 23−93.

(3) Catalioto, R.-M.; Criscuoli, M.; Cucchi, P.; Giachetti, A.; Giannotti, D.; Giuliani, S.; Lecci, A.; Lippi, A.; Patacchini, R.; Quartara, L.; Renzetti, A. R.; Tramontana, M.; Arcamone, F.; Maggi, C. A. MEN 11420 (Nepadutant), a novel glycosylated bicyclic peptide tachykinin NK-2 receptor antagonist. *Br. J. Pharmacol.* **1998**, *123*, 81−91.

(4) Giannotti, D.; Perrotta, E.; Di Bugno, C.; Nannicini, R.; Harmat, N. J. S.; Giolitti, A.; Patacchini, R.; Renzetti, A. R.; Rotondaro, L.; Giuliani, S.; Altamura, M.; Maggi, C. A. Discovery of Potent Cyclic Pseudopeptide Human Tachykinin NK-2 Receptor Antagonists. *J. Med. Chem.* **2000**, *43* (22), 4041−4044.

(5) Giolitti, A.; Cucchi, P.; Renzetti, A. R.; Rotondaro, L.; Zappitelli, S.; Maggi, C. A. Molecular determinants of peptide and nonpeptide NK-2 receptor antagonists binding sites of the human tachykinin NK-2 receptor by site-directed mutagenesis. *Neuropharmacology* **2000**, *39*, 1422−1429.

(6) Emonds-Alt, X.; Vilain, P.; Goulaouic, P.; Proietto, V.; Van Broeck, D.; Advenier, C.; Naline, E.; Neliat, G.; Brelière, J.-C.; Le Fur, G. *Life Sci.* **1992**, *50*, PL101−PL106.

(7) Palczewski, K.; Takashi, K.; Tetsuya, H.; Behnke, C. A.; Motoshima, H.; Fox, B. A.; et al. Crystal Structure of Rhodopsin: A G Protein-Coupled Receptor. *Science* **2000**, *489*, 739−745.

(8) Pavone, V.; Lombardi, A.; Maggi, C. A.; Quartara, L.; Pedone, C. Conformational Rigidity versus Flexibility in a Novel Peptidic Neurokinin A Receptor Antagonists. *J. Pept. Sci.* **1995**, *41*, 236−240.

(9) Cramer, R. D., III; Patterson, D. E.; Bunce, J. D. Comparative Molecular Field Analysis (CoMFA). 1. Effect of Shape on Binding of Steroids to Carrier Proteins. *J. Am. Chem. Soc.* **1988**, *110*, 5959−5967.

(10) Waller, C. L.; Oprea, T. I.; Giolitti, A.; Marshall, G. R. Three-Dimensional QSAR of Human Immunodeficiency Virus (I) Protease Inhibitors. 1. A CoMFA Study Employing Experimentally-Determined Alignment Rules. *J. Med. Chem.* **1993**, *36*, 4152−4160.

(11) Heritage, T. W.; Lowis, D. R. Molecular Hologram QSAR. In *Rational Drug Design*; Parrill, A. L., Reddy, M. R., Eds.; ACS Symposium Series 719; American Chemical Society: Washington, DC, 2000; pp 212−225.

(12) Bellucci, F.; Carini, F.; Catalani, C.; Cucchi, P.; Lecci, A.; Meini, S.; Patacchini, R.; Quartara, L.; Ricci, R.; Tramontana, M.; Giuliani, S.; Maggi, C. A. Pharmacological profile of the novel mammalian tachykinin hemokinin 1. *Br. J. Pharmacol.* **2002**, *135*, 266−274.

(13) Patacchini, R.; Giuliani, S.; Turini, A.; Navarra, G.; Maggi, C. A. Effect of nepadutant at tachykinin NK₂ receptors in human intestine and urinary bladder. *Eur. J. Pharmacol.* **2000**, *398*, 389−397.

(14) Gershengorn, M. C.; Osman, R. Minireview: Insights into G Protein-Coupled Receptor Function Using Molecular Models. *Endo* **2001**, *142* (1), 2−10.

(15) Hipskind, P. A.; Howbert, J. J.; Cho, S.; Cronin, J. S.; Fort, S. L.; Ginah, F. O.; Hansen, G. J.; Huff, B. E.; Lobb, K. L.; et al. Practical and Enantiospecific Synthesis of LY303870, a Novel NK-1 Antagonist. *J. Org. Chem.* **1995**, *60*, (21), 7033−7036.

(16) Giorgi, R.; Di Bugno, C.; Giannotti, D.; Maggi, C. A. Monocyclic compounds with four bifunctional residues having NK-2 antagonist action. PCT Int. Appl. WO 98 34949, Aug 13, 1998.